

EFFECT OF SUBSTRATES ON CRYSTAL STRUCTURES AND OPTICAL PROPERTIES OF WO₃ FILMS PREPARED BY THE POLYMERIC PRECURSOR METHOD

G. H. JIN, S. Q. LIU*

School of Chemistry and Chemical Engineering, Central South University, Changsha 410083 China

WO₃ thin films were prepared on three different substrates (Fluorine doped SnO₂ (FTO) coated glass, quartz glass and graphite substrates) by the polymeric precursor method involving the use of ammonium metatungstate as the precursor and polyethylene glycol as the structure-directing agent. The structure, morphological and optical properties of these films were studied using X-ray diffraction, Raman spectra, field emission scanning electron microscope, UV-vis transmission spectroscopy, and photoluminescence spectra techniques. X-ray diffraction analysis reveals that films prepared on graphite and quartz glass substrates are monoclinic structure, and those on FTO glass substrates are distorted cubic structure. The FESEM analysis shows that the WO₃ films on graphite substrate have adsorbed particles with voids and porous surface, whereas a compact and a granular structure with well defined grain boundaries were observed on films on FTO and quartz glass substrates. The values of the energy gap calculated from the absorption spectra are 2.61, 2.75 and 2.67 eV for WO₃ samples deposited onto graphite, FTO and quartz glass substrates, respectively. The films coated on graphite substrates have the strongest photoluminescence intensity of all the samples. The influence of substrate on the structure, morphological, and optical properties of the WO₃ films is discussed in the present paper.

(Received April 15, 2016; Accepted July 23, 2016)

Keywords: Tungsten oxide; Thin films; Substrates; Optical properties; Polymeric precursor method

1. Introduction

Tungsten trioxide (WO₃) is an n-type semiconductor, with a wide band gap of 2.6 eV at 300 K. Because of its excellent electrochromic, photochromic and gasochromic properties, WO₃ thin film has been used in a wide range of optical, chemical and electrical applications, including gas and temperature sensing, photocatalysis, electrochromic windows and displays, as well as flat panel displays [1-7]. In the last years, a large variety of methods have been employed for the preparation of transparent and conducting WO₃ thin films, such as vacuum evaporation [8], reactive sputtering [9], chemical vapor deposition (CVD) [4, 10], anodization [11, 12], electrodeposition [13, 14] and sol-gel precipitation [3, 15, 16]. The sol-gel technique has attracted great attention because of its various advantages, such as good homogeneity, ease of composition control, lower cost and larger area thin films than other techniques.

Many phases have been detected in the WO₃ system, such as hexagonal, pyrochlore, or distorted cubic [17, 18], all of which are comprised of corner- and/or edge-shared WO₆ octahedra [19]. In most cases, the annealing and photocatalytic property tests are performed between 200 °C and 500 °C. In this temperature range, WO₃ crystals undergo structural changes. It is reported that the crystal structure of WO₃ film is dependent on the preparation methods,

*Corresponding author: suqinliu@foxmail.com

annealing conditions and substrates for the films[20, 21], which is probably different from the bulk WO_3 . As described previously, the substrates play a significant role in the preparation of WO_3 films for their crystal structure and surface morphology[2, 22, 23]. However, until now the literature does not, to the best of our knowledge, cover an investigation comparing the influence of the substrates on the optical properties of the WO_3 thin films.

In the present paper, we studied the structural and optical characteristics of WO_3 thin films which could be used as a chemical sensor. WO_3 thin films coated on three different substrates (Fluorine doped SnO_2 (FTO) coated glass, quartz glass and graphite substrates) were prepared by a sol-gel method involving the use of ammonium metatungstate as the precursor and polyethylene glycol as the structure-directing agent. The substrate materials for our study were selected with respect to chemical stability (inertness in the high temperature) and high surface quality, to obtain films with high surface quality. The effect of using different substrates on crystal structures and optical properties of WO_3 thin films was studied.

2. Experiments

2.1. Materials preparation

At room temperature, 1.887 g ammonium metatungstate ($(\text{NH}_4)_6\text{W}_7\text{O}_{24}\cdot 6\text{H}_2\text{O}$, Sinoreagent, China) was dissolved in 10 ml deionized water and 0.944 g polyethylene glycol (PEG 1000, Sinoreagent, China) was added as a surfactant under magnetic stirring for 12 h, the precursor solution was partially evaporated under reduced pressure to reach a W concentration of ca. 0.5 mol/dm³.

After achieving complete dissolution of the precursor, it was cast on FTO glass, quartz glass and graphite substrates by the dip coating method with a pulling rate of 3 mm/s, respectively. The substrates were cleaned using acetone, ethanol and distilled water by ultrasonication before coating. The coated film was dried at room temperature followed and calcined in air at 450 °C for 3 h to form a WO_3 film.

2.2. Characterization

The crystalline phases of the WO_3 films were determined by an X-ray diffractometer (D/Max2250, Rigaku Corporation, Japan) using graphite monochromatic copper radiation (Cu K α , $\lambda=0.154056$ nm) at 40 kV, 300 mA. Raman spectra were obtained on a Renishaw RM2000 Raman spectrometer with 514.5 nm wavelength and 20 mW beam power. Morphologies of films were investigated by a field-emission scanning electron microscope (JSM6700F, JEOL Company, Japan). UV-visible diffuse reflectance (DR) spectra, in the 300–600 nm wavelength range, were obtained with a Shimadzu 2450 spectrophotometer. The PL spectra were recorded at room temperature by a HITACH-850; in the measurement, 245 nm line of the Xe lamp was used as exciting laser.

3. Results and discussion

The WO_3 films were synthesized from ammonium metatungstate as a precursor. PEG was used as a surfactant to bind tungsten species and a structure-directing agent to form a nanostructured film. Fig. 1 shows the XRD spectra for the WO_3 films coated on different substrates after the samples were calcined at 450 °C. The XRD patterns of the WO_3 powder prepared from polymeric precursor calcined at 450 °C for 3 h was also measured. As shown in Fig. 1, films coated on FTO glass show sharp diffraction peaks at 23.4 °, 34.0 °, 42.1 °, 49.0 ° and 55.3 °, which indicate cubic WO_3 phase according to JCPDS data (JCPDS 41-0905). The calculated lattice parameter of 0.3686 nm, is slightly shorter than the JCPDS lattice parameter ($a=0.3714$ nm). Since the cubic WO_3 is metastable, this difference can be assigned to the beginning of the transformation from cubic to monoclinic, such as observed by K. G. Varghese et al[24].

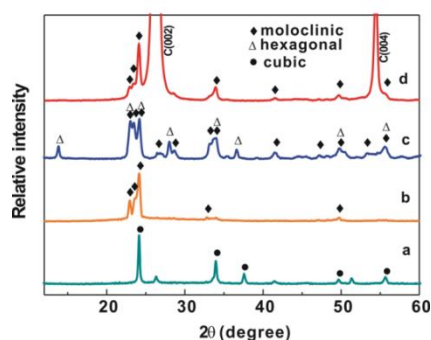


Fig. 1 X-ray diffraction patterns of WO_3 films coated on (a) FTO glass; (b) quartz glass; (d) graphite substrate; (c) WO_3 powders prepared from polymeric precursor.

For the films on both the quartz glass and graphite substrates, the diffraction patterns show three peaks in the region 23° - 25° (Fig. 1b and 1d), suggesting monoclinic structure in a main phase of WO_3 films. In addition, the diffraction of such films is consistent with strong preferential orientation of (200), (020), and (002) faces of WO_3 crystallites parallel to the substrate. Nishide et al. [22] have reported that a cubic crystal of WO_3 was formed on quartz glass substrate but a mixture of cubic and monoclinic crystals was formed on silicon wafers under the same firing conditions. Differences in these results might be attributed to the different synthetic method used in our study. The above-discussed XRD data shows clearly that the substrate strongly affects the process of the subsequent WO_3 films formation occurring during the heat treatment.

Moreover, as shown in Fig. 1c, except three large peaks in the region 23° - 25° are observed for the WO_3 powders calcined at 450°C , there is a small peak near $2\theta=14^\circ$, indicating the powders contain hexagonal structure WO_3 and monoclinic structure WO_3 simultaneously. Some researchers have reported that the XRD patterns of WO_3 powders are different from those of the corresponding films [25, 26].

The room temperature Raman spectra of the WO_3 films on various substrates are shown in Fig. 2. As shown in Fig. 2b and 2c, the films coated on quartz glass and graphite substrates exhibited the similar spectrum profile. Two broad bands were clearly detected: high in the 740 - 980 cm^{-1} region and low in the 200 - 400 cm^{-1} . The two peaks observed at 715 and 805 cm^{-1} are attributed to the symmetric and asymmetric vibration of W^{6+} -O bonds (O-W-O stretching modes). Two peaks centered at 322 and 266 cm^{-1} can be found in the 200 - 400 cm^{-1} range and correspond to W-O-W bending modes of the bridging oxygen. These broad bands observed in the Raman spectrum of films on quartz glass and graphite substrates agree with that of monoclinic WO_3 reported in film samples by Santato [3]. The spectrum of the films on FTO glass had a tendency to shift, with well-defined Raman bands at 255 , 293 , 707 , 795 cm^{-1} . This discrepancy might arise from a distorted cubic structure WO_3 , which transformed to monoclinic WO_3 . This result is consistent with X-ray diffraction measurements. However, we had not observed the bands at 413 cm^{-1} , which is corresponding to distorted octahedra as reported by Fery et al [27]. This might be ascribed to the different precursor and substrates used in our study.

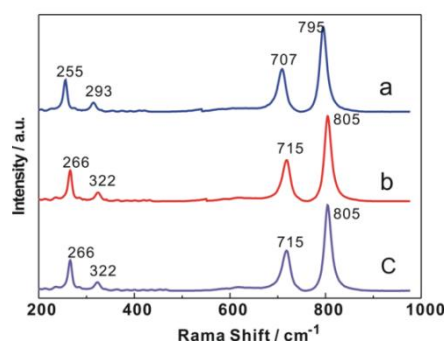


Fig. 2 Raman shift spectra of WO_3 films on (a) FTO glass; (b) quartz glass; (c) graphite substrate calcined at 450°C .

Fig. 3 shows the FESEM micrographs of WO_3 films grown on various substrates. The WO_3 films coated on graphite substrate show adsorbed particles with voids and porous surface, whereas a compact and a granular structure with well defined grain boundaries were observed on films on FTO and quartz glass substrates. For FTO and quartz glass substrates, there were no adsorbed colloidal particles, and a remarkable uniform grain size was observed indicating that there was a uniform nucleation throughout the substrate surface. Smooth surfaces lead to a more uniform, fine grain structure while rough surfaces with more peaks and valleys lead to an open and porous type microstructure.

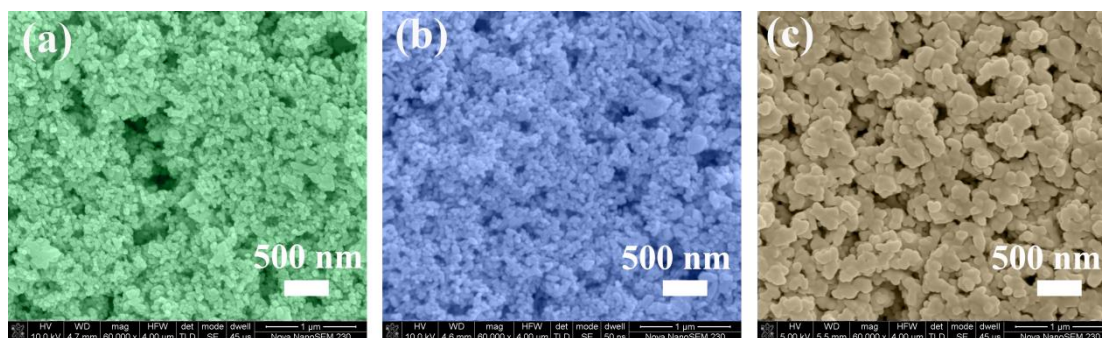


Fig. 3 Field emission scanning electron micrographs WO_3 films (a) FTO glass; (b) quartz glass; (c) graphite substrate calcined at 450°C .

We investigated the UV-vis absorption spectra for WO_3 thin film deposited on graphite substrate (inset in Fig. 4). The onset position of light absorption for the sample is around 470 nm. Considering WO_3 is an indirect semiconductor, a plot of the modified Kubelka-Munk function versus the energy of exciting light for the WO_3 film is shown in Fig. 4, affording band gap energy of 2.61 eV for the WO_3 films deposited on graphite substrate. This optical band gap value is in good agreement with the values obtained for bulk WO_3 crystals [28].

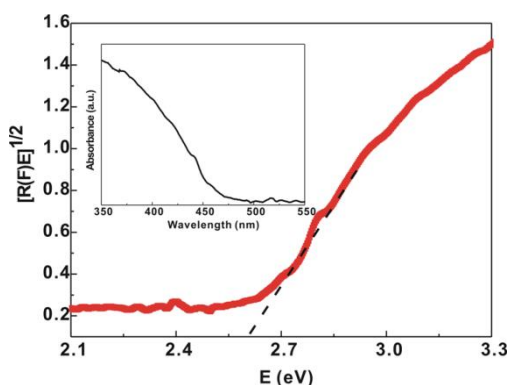


Fig. 4 UV-vis absorption spectra of WO_3 films on graphite substrate calcined at $450\text{ }^\circ\text{C}$.

The optical transmission spectra of the films coated on FTO and quartz glass substrates for a wavelength range of 300-900 nm are shown in Fig. 5. It is shown that the transmittivities of the films deposited on FTO and quartz glass substrates were about 90% in the visible range. The oscillations in the transmission spectra are caused by optical interference arising ascribe to the interference of multiple reflections originated from film and substrate surfaces and difference of refractive index of films with substrate. In addition, the transmittance improved when the films were deposited on FTO glass substrates, particularly in shorter wavelength.

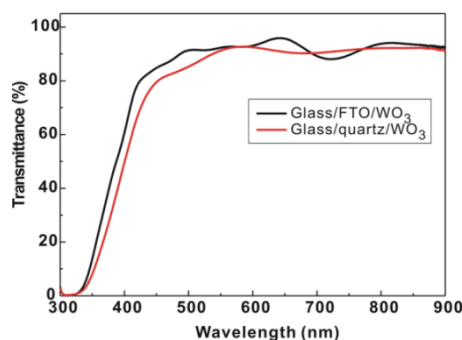


Fig. 5 Transmission spectra for WO_3 films on FTO glass and quartz glass calcined at $450\text{ }^\circ\text{C}$.

The band gap, E_g of the WO_3 films coated on FTO and quartz glass substrates was estimated from the UV-vis absorption spectra. Using the film thickness (d) and the measured spectral transmittance (T), the absorption coefficient (α) can be calculated using the expression[29]:

$$\alpha = \frac{1}{d} \left[\frac{1-R^2}{T} \right] \quad (1)$$

Where R is the reflection coefficient from the sample assumed to be zero. The optical band gap was determined using the Tauc formula[29]:

$$\alpha h\nu = A(h\nu - E_g)^n \quad (2)$$

Where $h\nu$ is the incident photon energy, A is a constant, E_g represents the energy band gap and the exponent n depends on the kind of optical transition. For crystalline semiconductors, n can take

values of 1/2, 3/2, 2 or 3 when the transitions are direct allowed, direct forbidden, indirect allowed and indirect forbidden transitions, respectively[30]. The value of $n = 2$ for the indirect allowed transition is found to be most suitable for the films prepared on FTO and quartz glass substrates because it gives the best linear graph in the band edge region. Fig. 6 shows the plot of $(\alpha hv)^{1/2}$ vs. hv for the films on FTO and quartz glass substrates. An extrapolation of the straight line to the linear portion of the curve to photon energy axis gives the value of band gap. It is known that the fundamental absorption limit for WO_3 mono-crystals is situated around 2.70 eV. As shown in Fig. 6, the indirect band gap values of the WO_3 films deposited on FTO and quartz glass substrates were estimated to be 2.75 eV and 2.67 eV, respectively.

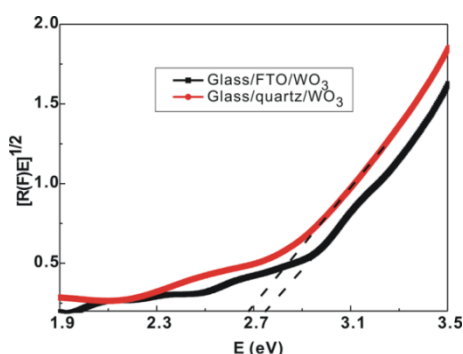


Fig. 6 Spectral dependence of the absorption coefficient, $(\alpha hv)^{1/2} = f(hv)$, for WO_3 samples deposited onto FTO glass and quartz glass.

Little is known about the photoluminescence of nanostructured WO_3 films. Fig. 7 shows the room-temperature PL emission spectra (excitation at 275 nm) of the WO_3 films deposited on various substrates. Strong blue emission for all films was observed between 460–500 nm, which might originate from the presence of oxygen vacancies or defects, as proposed by Lee[31]. A very clear emission peak at 472 nm was observed in the PL spectra of films coated on quartz glass and graphite substrates, while a PL emission peak was observed at 475 nm from films coated on FTO glass, with a slight blue-shift. Compared with the emission peak of the films on FTO glass, the emission intensity of the films on quartz glass is higher, and the intensity of the films on graphite substrates is the strongest of all the samples. Since the films on FTO and quartz glass had a similar particle size, the results indicate that the photoluminescence of the WO_3 films coated on various substrates is not only size-dependent, but also connected with the structure of WO_3 .

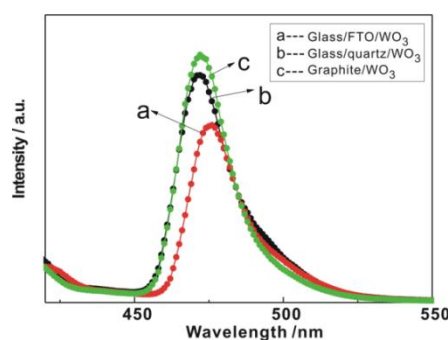


Fig. 7 PL spectra of WO_3 films on FTO glass, quartz glass and graphite substrate calcined at 450 °C.

At one hand, it is known that the scattering efficiencies of larger particles are larger than those of smaller particles[32, 33]. Light absorption efficiency is enhanced attribute to lengthening of photon propagation distance in films by large particle scattering effects, which will increase photon absorption rate. Therefore, the enhanced light absorption will increase the emission intensity of photoluminescence. In our experiment, the grain size of the films deposited on graphite substrate was larger than that on glass quartz from the SEM images. The XRD data shows that both films on quartz glass and graphite substrates were monoclinic structures, thus the films on graphite substrates had a stronger PL emission intensity because of their larger WO_3 particles.

On the other hand, the films on FTO and quartz glass were cubic and monoclinic WO_3 , respectively, and both of them had a similar particle size, about 50 nm. However, the lowest emission intensity was observed for thin films on FTO glass. This might be attributed to the different crystal structure of WO_3 films on FTO and quartz glass.

In a simplified description, the structure of WO_3 may be regarded as a modification of the perovskite-type ABO_3 lattice in which the A site remains unoccupied and the W atoms occupy the B site. This produces a three-dimensional crystalline network of corner-shared octahedra WO_6 [34-38]. It is known that the structure of monoclinic WO_3 (m- WO_3) belongs to the space group $\text{P}21/n$ in which each tungsten atom is surrounded by six oxygen atoms in an octahedral coordination. As shown in Fig. 8A, every four WO_6 octahedra in the unit cell of m- WO_3 are slightly tilted with respect to one other. Therefore, the structure of m- WO_3 is less symmetrical as compared with that of ReO_3 type. Nevertheless, the ideal cubic WO_3 structure can be represented as a cubic ReO_3 structure, which consists of a three-dimensional network of corner-sharing WO_6 octahedra, as shown in Fig. 8B.

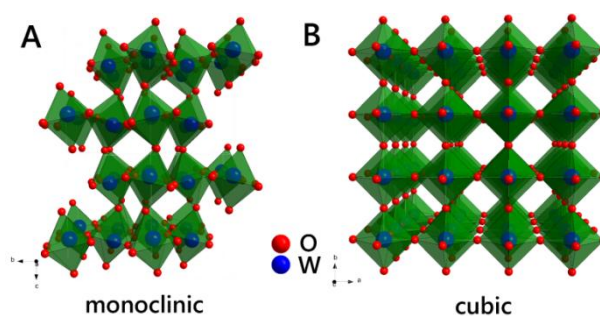


Fig. 8 Perspective views of the crystal structures of (A) monoclinic and (B) cubic WO_3 .

It was found that some of WO_3 properties like electrochromic or catalytic ones are obviously connected with the crystal structure[39, 40]. Some literatures have demonstrated that the tunnels surrounded by WO_6 octahedra play a key role in the kinetic behavior [39, 41]. Hence, the different photoluminescence intensity of thin films on FTO and quartz glass can be assigned to the different tunnel structures, as shown in Fig. 8.

4. Conclusions

The comparison of the properties of WO_3 with respect to the used substrate material (FTO glass, quartz glass and graphite substrates) shows that there is a dependency on the substrate material with respect to the surface morphology, crystallinity, composition, and optical properties of the resulting films. The films prepared on graphite and quartz glass substrates are monoclinic structure, and those on FTO glass substrates are distorted cubic structure. All WO_3 thin films showed a high transmittance in the visible region. The values of the energy gap calculated from the absorption spectra are 2.61, 2.75 and 2.67 eV for WO_3 sample deposited onto graphite, FTO and quartz glass substrates, respectively. The PL results show that the photoluminescence properties of WO_3 film were size-dependence and related to the crystal structures on the different substrates.

Acknowledgments

This study was supported by the Fundamental Research Funds for the Central Universities of Central South University (grants no. 2014zzts016)

References

- [1] B. Yang, Y. Zhang, E. Drabarek, P.R.F. Barnes, V. Luca, *Chem. Mater.*, **19**, 5664(2007).
- [2] S. Wang, T. Chou, C. Liu, *Sensors and Actuators B*, **94**, 343(2003).
- [3] C. Santato, M. Odziemkowski, M. Ulmann, J. Augustynski, *J. Am. Chem. Soc.*, **123**, 10639(2001).
- [4] R. Sivakumar, A. Moses Ezhil Raj, B. Subramanian, M. Jayachandran, D. Trivedi, C. Sanjeeviraja, *Mater. Res. Bull.*, **39**, 1479(2004).
- [5] M. Deepa, R. Sharma, A. Basu, S.A. Agnihotry, *Electrochim. Acta*, **50**, 3545(2005).
- [6] H. Habazaki, Y. Hayashi, H. Konno, *Electrochim. Acta*, **47**, 4181(2002).
- [7] M. Gratzel, *Nature*, **409**, 575(2001).
- [8] R. Colton, A. Guzman, J. Rabalais, *J. Appl. Phys.*, **49**, 409(1978).
- [9] D. Le Bellac, A. Azens, C. Granqvist, *Appl. Phys. Lett.*, **66**, 1715(1995).
- [10] B. Yous, S. Robin, A. Donnadiou, G. Dufour, C. Maillot, H. Roulet, C. Senemaud, *Mater. Res. Bull.*, **19**, 1349(1984).
- [11] H. Tsuchiya, J. Macak, I. Sieber, L. Taveira, A. Ghicov, K. Sirotna, P. Schmuki, *Electrochem. Commun.*, **7**, 295(2005).
- [12] S. Berger, H. Tsuchiya, A. Ghicov, P. Schmuki, *Appl. Phys. Lett.*, **88**, 203119 (2006).
- [13] S.-H. Baeck, K.-S. Choi, T.F. Jaramillo, G.D. Stucky, E.W. McFarland, *Adv. Mater.*, **15**, 1269(2003).
- [14] M. Yagi, S. Umemiya, *J. Phys. Chem. B*, **106**, 6355(2002).
- [15] H. Wang, T. Lindgren, J. He, A. Hagfeldt, S. Lindquist, *J. Phys. Chem. B*, **104**, 5686(2000).
- [16] C. Santato, M. Ulmann, J. Augustynski, *Adv. Mater.*, **13**, 511(2001).
- [17] C. Genin, A. Driouiche, B. Gérard, M. Figlarz, *Solid State Ionics*, **53-56**, 315.
- [18] J.-D. Guo, K.P. Reis, M. Stanley Whittingham, *Solid State Ionics*, **53-56**, 305(1992).
- [19] B. Ingham, S.V. Chong, J.L. Tallon, *J. Phys. Chem. B*, **109**, 4936(2005).
- [20] A. Al Mohammad, M. Gillet, *Thin Solid Films*, **408**, 302(2002).
- [21] C. Ramana, S. Utsunomiya, R. Ewing, C. Julien, U. Becker, *J. Phys. Chem. B*, **110**, 10430(2006).
- [22] T. Nishide, F. Mizukami, *Thin Solid Films*, **259**, 212(1995).
- [23] C. Balázsi, L. Wang, E.O. Zayim, I.M. Szilágyi, K. Sedlacková, J. Pfeifer, A.L. Tóth, P.-I. Gouma, *J. Eur. Ceram. Soc.*, **28**, 913(2008).
- [24] K.G. Varghese, V.K. Vaidyan, *AIP Conf Proc*, **1075**, 121(2008).
- [25] B. Ohtani, T. Atsumi, S. Nishimoto, T. Kagiya, *Chem. Lett.*, **17**, 295(1988).
- [26] L. Palatnik, O. Obolyaninova, M. Naboka, N. Gladkikh, *Inorg. Mater*, **9**, 801(1973).
- [27] G.L. Frey, A. Rothschild, J. Sloan, R. Rosentsveig, R. Popovitz-Biro, R. Tenne, *J. Solid State Chem.*, **162**, 300(2001).
- [28] C. Granqvist, *Handbook of inorganic electrochromic materials*, Elsevier Science Ltd (1995).
- [29] H. JN, *Optical absorption and dispersion in solids*, CRC Press (1970).
- [30] J. Pankove, *Optical processes in semiconductors*, Dover publications (1975).
- [31] K. Lee, W. Seo, J. Park, *J. Am. Chem. Soc.*, **125**, 3408(2003).
- [32] A. Usami, *Chem. Phys. Lett.*, **277**, 105(1997).
- [33] A. Usami, *Sol. Energ. Mat. Sol. C.*, **64**, 73(2000).
- [34] M. Kawaminami, T. Hirose, *J. Phys. Soc. Jpn.*, **46**, 864(1979).
- [35] G.M. Ramans, J.V. Gabrusenoks, A.R. Lusic, A.A. Patmalnieks, *J. Non-cryst. Solids.*, **90**, 637(1987).
- [36] A. Hjelm, C.G. Granqvist, J.M. Wills, *Phys. Rev. B*, **54**, 2436(1996).

- [37] L.A. Bursill, *J. Solid State Chem.*, **48**, 256(1983).
- [38] M. Kawaminami, T. Hirose, *J. Phys. Soc. Jpn.*, **47**, 1733(1979).
- [39] S. Komaba, N. Kumagai, K. Kato, H. Yashiro, *Solid State Ionics*, **135**, 193(2000).
- [40] I.M. Szilágyi, S. Saukko, J. Mizsei, A.L. Tóth, J. Madarász, G. Pokol, *Solid State Sci.*, **12**, 1857(2010).
- [41] A. Yu, N. Kumagai, H. Yashiro, *Solid State Ionics*, **100**, 267(1997).